2136 J. Med. Chem. 2010, 53, 2136–2145
DOI: 10.1021/jm901660c

Journal of Medicinal Chemistry Article

# Design, Synthesis, and Evaluation of 2-Methyl- and 2-Amino-*N*-aryl-4,5-dihydrothiazolo-[4,5-*h*]quinazolin-8-amines as Ring-Constrained 2-Anilino-4-(thiazol-5-yl)pyrimidine Cyclin-Dependent Kinase Inhibitors†

Neil A. McIntyre,[‡,∥] Campbell McInnes,[§,∥,⊥] Gary Griffiths,[§] Anna L. Barnett,[§] George Kontopidis,[§,#] Alexandra M. Z. Slawin,[‡] Wayne Jackson,[§] Mark Thomas,[§] Daniella I. Zheleva,[§] Shudong Wang,[§,∞] David G. Blake,*[,§] Nicholas J. Westwood,*[,‡] and Peter M. Fischer*[,§,∞]

[‡]*School of Chemistry and Biomedical Sciences Research Complex, University of St. Andrews, North Haugh, St. Andrews, Fife KY16 9ST, U.K., and* [§]*Cyclacel Limited, 1 James Lindsay Place, Dundee DD1 5JJ, U.K.* [∥]*These authors contributed equally to the work presented.* [⊥]*Present address: South Carolina College of Pharmacy, CLS 514, 715 Sumter Street, University of South Carolina, Columbia, South Carolina 29208.* [#]*Present address: Biochemistry Laboratory, Veterinary School, University of Thessaly, Karditsa 43100, Greece.* [∞]*Present address: School of Pharmacy and Centre for Biomolecular Sciences, University of Nottingham, University Park, Nottingham NG7 2RD, U.K.*

*Received November 10, 2009*

Following the recent discovery and development of 2-anilino-4-(thiazol-5-yl)pyrimidine cyclin dependent kinase (CDK) inhibitors, a program was initiated to evaluate related ring-constrained analogues, specifically, 2-methyl- and 2-amino-*N*-aryl-4,5-dihydrothiazolo[4,5-*h*]quinazolin-8-amines for inhibition of CDKs. Here we report the rational design, synthesis, structure−activity relationships (SARs), and cellular mode-of-action profile of these second generation CDK inhibitors. Many of the analogues from this chemical series inhibit CDKs with very low nanomolar $K_i$ values. The most potent compound reported in this study inhibits CDK2 with an $IC_{50}$ of 0.7 nM ([ATP] = 100 $\mu$M). Furthermore, an X-ray crystal structure of 2-methyl-*N*-(3-(nitro)phenyl)-4,5-dihydrothiazolo[4,5-*h*]quinazolin-8-amine (**11g**), a representative from the chemical series in complex with cyclin A−CDK2, is reported, confirming the design rationale and expected binding mode within the CDK2 ATP binding pocket.

## Introduction

CDKs[a] fulfill two main regulatory roles in the human cell. They control progression through the cell proliferation cycle, and they are also important in the regulation of transcription through phosphorylation of the C-terminal domain (CTD) of RNA polymerase-II (RNAP-II).[1] In human cancers, genetic and epigenetic aberrations frequently result in overexpression of cyclins or suppression of CDK-inhibitory tumor suppressor proteins (CDKIs), which provides tumor cells with a selective growth advantage.[2,3] Ectopic expression of CDKIs in tumor cells restores cell cycle control, usually causing arrest in the gap phases that precede and follow the DNA-synthesis phase. In addition, in some cell systems, expression of CDKIs leads to apoptosis.[4] However, the observation that transformed cells, and even some untransformed cells, that lack cyclin E or CDK2 continue to proliferate[5−7] raises the possibility that the specific targeting of individual cell cycle CDKs may not be an optimal therapeutic strategy because of the inherent functional redundancy of these kinases.[8]

An alternative approach is to explore the potential therapeutic benefit of targeting those CDKs that are involved in the regulation of transcription. The largest subunit of RNAP-II contains a CTD domain that is composed of a repeating heptad sequence of amino acids. The phosphorylation status of the Ser residues at positions 2 and 5 of the heptad has been shown to be important in the activation of RNAP-II. A number of kinases have been reported to phosphorylate the CTD of RNAP-II, but the most important ones appear to be CDK7−cyclin H and CDK9−cyclin T.[9,10] CDK7−cyclin H acts as a CDK-activating kinase (CAK) for other CDKs and also associates with the RING-finger protein MAT1 in the general transcription factor IIH (TFIIH). Various studies have identified Ser-5 of the CTD as its preferred substrate site.[11] CDK9, in association with cyclin T1, T2, or K, exists with numerous other partners in a complex known as positive transcription elongation factor b (P-TEFb)[12] and has been shown to phosphorylate both Ser-2 and Ser-5 of the CTD heptad.[13] Phosphorylation of these Ser residues provides the stimulus for efficient initiation and elongation of mRNA synthesis by the RNAP-II transcriptional complex. Although there is contradictory evidence regarding the

†X-ray crystallography data were deposited at the PDB database (code 2X1N).

*To whom correspondence should be addressed. For D.G.B. (cyclacel): phone, +44-1382-206062; fax, +44-1382-206067; e-mail, dblake@cyclacel.com. For N.J.W. (chemistry): phone, +44-1334-463816; fax, +44-1334-463808; e-mail, njw3@st-andrews.ac.uk. For P.M.F.: phone, +44-115-8466242; fax, +44-115-9513412; e-mail, peter.fischer@nottingham.ac.uk.

[a]Abbreviations: Bredereck's reagent, *tert*-butoxybis(dimethylamino)-methane; CAK, cyclin-dependent-kinase-activating kinase; CDK, cyclin dependent kinase; DDQ, 2,3-dichloro-5,6-dicyano-1,4-benzoquinone; DMF-DMA, *N*,*N*-dimethylformamide dimethyl acetal; MTT, (3-(4,5-dimethylthiazol-2-yl)-2,5-diphenyltetrazolium bromide; $Pd_2(dba)_3$, tris-(dibenzylideneacetone)dipalladium(0); pRb, retinoblastoma protein; P-TEFb, positive transcription elongation factor b; RNAP-II CTD, RNA polymerase-II C-terminal domain; SAR, structure−activity relationship; TFIIH, general transcription factor IIH; TUNEL, terminal deoxynucleotidyl transferase-mediated nick end labeling; xantphos, 4,5-bis(diphenylphosphino)-9,9-dimethylxanthene.

 Published on Web 02/10/2010 

absolute specificity of CDK7−cyclin H and CDK9−cyclin T1 for each Ser residue of the CTD, consensus exists about the importance of these CDKs in the regulation of RNAP-II activity and hence in the control of transcription.[1,14,15] CDK1, CDK2, CDK8, and CDK11 have also been implicated in the phosphorylation of RNAP-II, but much less is known regarding the roles of these CDKs in transcriptional regulation.[13]

At least two of the experimental CDK inhibitor drugs that are currently undergoing clinical development, flavopiridol (alvocidib; Aventis/NCI) and *R*-roscovitine (seliciclib, CYC202; Cyclacel), are believed to owe their anticancer activity predominantly to the transcriptional inhibition mechanism.[16] The apparent specificity against tumor versus normal proliferating cells of transcriptional CDK inhibitors is believed to be due to the fact that transformed cells selectively depend on sustained transcription of antiapoptotic and prosurvival genes in order to resist oncogene-induced susceptibility to apoptosis.[17,18]

We have previously described various 2-anilino-4-heteroarylpyrimidines as CDK inhibitors, including 2-anilino-4-(4-methyl-thiazol-5-yl)pyrimidines **1a** ($R^1$ = Me; Figure 1).[19−22]

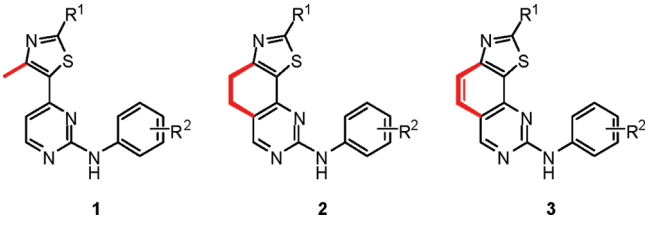


**Figure 1.** 2-Anilino-4-(4-methylthiazol-5-yl)pyrimidine **1**, (4,5-dihydro-thiazolo[4,5-*h*]quinazolin-8-yl)aniline **2**, and thiazolo[4,5-*h*]quinazolin-8-yl-aniline **3** CDK inhibitors.

Here we report on the design, synthesis, and characterization of conformationally constrained analogues of **1**, i.e., *N*-aryl-4,5-dihydrothiazolo[4,5-*h*]quinazolin-8-amines **2**, as well as their fully aromatic counterparts **3**.

## Chemistry

Compounds that can be regarded as ring-constrained analogues of **1** (Figure 1), i.e., **2** and **3**, were prepared as outlined in Scheme 1. Retrosynthetic analysis of **2** suggested cyclohexane-1,3-dione **4** as a suitable starting material, based on the usual thiazole and aminopyrimidine preparation methods.[23,24] Bromination of **4** provided the intermediate α-bromodiketone **5**.[23,24] Heating **5** with thioacetamide (**6a**, $R^1$ = Me) in pyridine or thiourea (**6b**, $R^1$ = $NH_2$) in pyridine−methanol, respectively, afforded the 2-substituted-5,6-dihydro-4*H*-benzothiazol-7-ones **7** following purification by distillation (**7a**) or crystallization (**7b**).[23] The primary amino group of the product **7b** was found to interfere in subsequent reactions and was therefore blocked as the acetamide **7c**. The cyclohexanone ring in **7** was next formylated, using a large excess of both sodium methoxide and freshly distilled ethyl formate to provide the enol products **8**. In the case of **7a** it was found that fresh sodium methoxide (generated in situ from sodium hydride and methanol) gave the best results in the production of **8a**. Although **8a** can be used in a number of heterocyclic ring formation reactions directly,[25−27] pilot condensation reactions with a number of guanidines showed that the 1,3-dicarbonyl function in **8a** was not sufficiently reactive for the intended purposes. We therefore converted **8** to enaminone **9** derived from morpholine, which we envisaged would be more reactive and less susceptible to degradation in the pyrimidine ring formation reactions. The

**Scheme 1.** Synthesis of Ring-Constrained 2-Anilino-4-(thiazol-5-yl)pyrimidines[a]

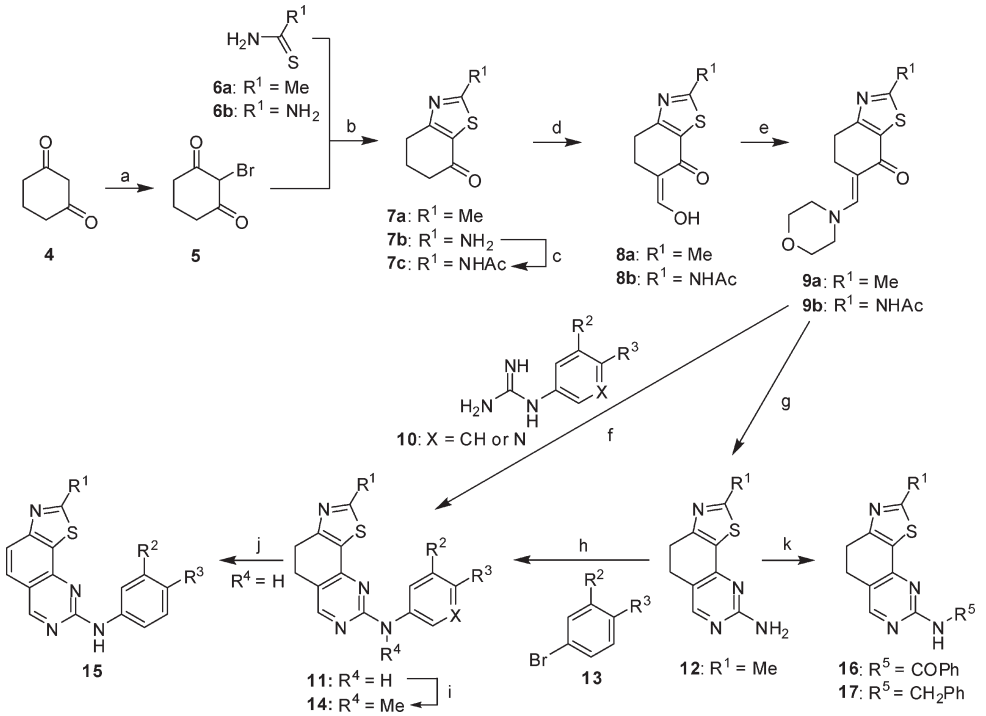


[a] Reagents: (a) $Br_2$, $CH_2Cl_2$; (b) pyridine (**7a**), pyridine−MeOH (**7b**); (c) $Ac_2O$; (d) ethyl formate, NaOMe, $Et_2O$/THF; (e) morpholine, PhMe; (f) NaOH, 2-methoxyethanol; (g) guanidine hydrochloride, NaOH, EtOH; (h) $Pd_2(dba)_3$, 4,5-bis(diphenylphosphino)-9,9-dimethylxanthene (xantphos), $Cs_2CO_3$, 1,4-dioxane; (i) MeI, NaH, DMF; (j) 2,3-dichloro-5,6-dicyano-1,4-benzoquinone (DDQ), PhMe; (k) benzoyl chloride, pyridine (**16**); benzyl bromide, LHMDS, THF (**17**).

**Table 1.** Structures of Constrained Thiazolopyrimidines and Summary of CDK Inhibitory Activity

| | structure[a] | | | | | | CDK inhibition, $K_i$ ($\mu$M)[b] | | | | |
|---|---|---|---|---|---|---|---|---|---|---|---|
| compd[a] | $R^1$ | $R^2$ | $R^3$ | $R^4$ | $R^5$ | X | 1B | 2E | 4D | 7H | 9T |
| **11a** | Me | H | H | H | | CH | 0.75 | 0.001 | 0.90 | 2.2 | 0.26 |
| **11b** | $NH_2$ | H | H | H | | CH | 0.63 | 0.088 | 0.33 | 1.2 | 0.11 |
| **11c** | Me | H | $CF_3$ | H | | CH | 0.96 | 0.16 | 4.9 | >10 | 1.9 |
| **11d** | Me | OH | H | H | | CH | 0.36 | 0.011 | 0.58 | 0.053 | 0.032 |
| **11e** | Me | H | OH | H | | CH | 0.20 | 0.001 | 0.54 | 0.30 | 0.49 |
| **11f** | Me | H | $NO_2$ | H | | CH | 0.31 | 0.13 | >10 | 4.8 | 0.14 |
| **11g** | Me | $NO_2$ | H | H | | CH | 0.32 | 0.023 | 2.0 | 0.79 | 0.002 |
| **11h** | $NH_2$ | $NO_2$ | H | H | | CH | 0.018 | 0.001 | 0.13 | 0.14 | 0.003 |
| **11i** | Me | H | $NMe_2$ | H | | CH | 2.5 | 0.010 | 0.037 | 0.060 | 0.64 |
| **11j** | Me | H | morpholine | H | | CH | 15 | 0.20 | >10 | 1.0 | 0.64 |
| **11k** | Me | H | OMe | H | | N | 0.078 | 0.049 | 0.12 | 1.1 | 1.0 |
| **11l** | Me | H | Cl | H | | N | 0.019 | 0.025 | 0.040 | 1.4 | 1.2 |
| **11m** | Me | H | COOMe | H | | CH | 0.70 | 0.92 | 2.4 | 6.3 | 0.67 |
| **12** | Me | | | | | | >10 | >10 | >10 | >10 | >10 |
| **11n** | $NH_2$ | H | $NMe_2$ | H | | CH | 0.098 | 0.031 | 0.47 | 0.50 | 0.16 |
| **14** | Me | $NO_2$ | H | Me | | CH | 2.7 | 0.59 | >10 | 1.8 | 12 |
| **15a** | Me | $NO_2$ | H | Me | | CH | 7.5 | 1.6 | >10 | >10 | >10 |
| **15b** | Me | H | H | H | | CH | 1.7 | 0.024 | 2.7 | >10 | >10 |
| **16** | Me | | | | COPh | | >10 | >10 | >10 | >10 | >10 |
| **17** | Me | | | | $CH_2Ph$ | | >10 | >10 | >10 | >10 | >10 |

[a] Refer to Scheme 1. [b] Determined as described in Experimental Methods (1B, CDK1−cyclin B; 2E, CDK2−cyclin E; 4D, CDK4−cyclin D1; 7H, CDK7−cyclin H−MAT1; 9T, CDK9−cyclin T1).

morpholinoenaminone formation reaction proceeded in high yield and afforded crystalline products **9a** and **9b**.

We also investigated direct dimethylaminoenaminone formation from **7a** and **7b** with the aid of *N*,*N*-dimethylformamide dimethyl acetal (DMF-DMA) or *tert*-butoxybis-(dimethylamino)methane (Bredereck's reagent).[28] These procedures did not offer any advantages because of poor reactivity in both the enaminone formation, as well as the subsequent pyrimidine ring formation steps. However, in the case of the starting material **7b**, temporary amino protection could be circumvented when DMF-DMA or Bredereck's reagent was employed, since excess of these reagents converted the amino group to the *N*,*N*-dimethylformamidine, which subsequently regenerated the free amine during pyrimidine ring formation, analogous to the corresponding transformation in the unconstrained thiazolepyrimidine series 1 (Figure 1).[20]

Pyrimidine ring formation was performed with the aid of arylguanidines **10**[20,29] under conditions similar to those developed for the synthesis of other 2-arylamino-4-(hetero)-arylpyrimidines.[20−22] In the case of **9b**, the acetamide group was hydrolyzed under the reaction conditions applied to furnish directly the desired pyrimidines **11** as the free amine ($R^1$ = $NH_2$). The limiting factor in the preparation of analogues **11** was nevertheless the efficiency of the heterocyclic condensation reactions between enaminones **9** and guanidines **10** to form the aminopyrimidine ring.[30,31] In contrast to the facile preparation of the corresponding unconstrained compounds,[20] under a range of conditions of auxiliary base, solvent, and temperature, the yields were generally low. Application of forcing conditions was observed to lead to decomposition, as evidenced by the formation of complex reaction mixtures. Reactivity and yields were dependent on the nature of the arylguanidines **10**, as expected. Whereas reaction of **9a** with phenylguanidine (**10**; $R^2$ = $R^3$ = H, X = CH) afforded the corresponding product **11a** (Table 1) in an isolated yield of 46%, ring-substituted guanidines generally gave lower yields (5−30%), with the notable exception of the *p*-dimethylaminophenylguanidine (**10**; $R^2$ = H, $R^3$ = $NMe_2$, X = CH), where product **11i** (Table 1) was obtained in 92% yield after purification. In general microwave irradiation was found to be a useful way of reducing reaction times and improving yields in the pyrimidine condensation reactions.

In order to improve the final yields in the synthesis of compounds with the general structure **11**, we sought alternative routes that would obviate the troublesome condensation between enaminones **9** and arylguanidines **10**. During the optimization of this latter reaction we were surprised to note that condensation of **9a** with unsubstituted guanidine hydrochloride afforded aminopyrimidine **12** in high yield (90%). This result led us to consider N-arylation reactions as an alternative approach in the synthesis of compounds **11**. Recently the palladium-catalyzed N-(hetero)arylation of some simple heteroarylamines, including 2-aminopyridine and 2-aminopyrimidine, has been reported.[32] The impressive yields reported for these C−N bond-forming reactions encouraged us to replicate the conditions developed by Yin and co-workers,[32] i.e., tris(dibenzylideneacetone)dipalladium(0) ($Pd_2(dba)_3$) as catalyst, 4,5-bis(diphenylphosphino)-9,9-dimethylxanthene (xantphos) as ligand, $Cs_2CO_3$ as base, and 1,4-dioxane as the solvent, in an attempt to couple aryl and heteroaryl bromide derivatives to aminopyrimidine **12**. Initial success with these reactions was achieved when using electron-deficient or neutral aryl bromide derivatives **13**, as we observed clean conversions of reactants to the corresponding products with associated high yields. However, when investigating the scope of this reaction further, we found that electron-rich aryl and heteroaryl bromides failed to react under similar conditions. Nevertheless, the palladium-catalyzed arylation reactions increased the overall yields in many cases and allowed us to scale up the production of the ring-constrained analogues **11**.

We next turned our attention to the synthesis of related analogues **14**−**17** in order to extend the SARs. N-Methylation of compound **11g** using sodium hydride and iodomethane gave **14**, which we envisaged as an inactive control compound. Surprisingly, the fully aromatic N-methylated 2-dimethyl-*N*-(3-nitrophenyl)thiazolo[4,5-*h*]quinazolin-8-amine

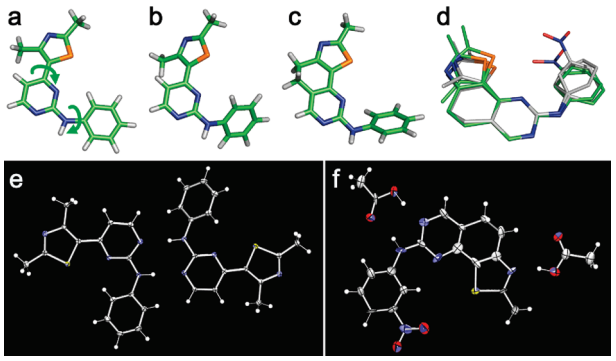


**Figure 2.** Typical CDK2-bound coplanar conformation of **1b** (a). The rotatable bonds linking the pyrimidine with the thiazole and phenyl rings are indicated by arrows. A likely low-energy solution conformation of **1b** is shown in (b). The conformational constraint provided by tethering the thiazol-4-yl methyl group to C5 of the pyrimidine is illustrated in (c). The single crystal structure conformations (gray CPK) are superimposed (based on the pyrimidine ring heavy atoms) on those observed in the CDK2 complexes (green CPK) of **1c**[20] and compound **11g** in (d). ORTEP (50% probability ellipsoids) diagrams for the single crystal structures of these compounds are shown in (e) and (f). For details refer to Supporting Information.

**15a** was also isolated from this reaction as a minor product. Although the mechanism of formation of this adventitious product has not been established, it encouraged us to try dehydrogenation reactions on compounds of type **11**. Indeed the formation of the fully aromatic 2-methyl-*N*-phenylthiazolo[4,5-*h*]quinazolin-8-amine **15b** from the related 4,5-dihydro analogue **11a** was successfully achieved using the reagent 2,3-dichloro-5,6-dicyano-1,4-benzoquinone (DDQ)[33] in refluxing toluene. Finally, in order to determine whether pyrimidine N2-substituent groups other than aryl could be tolerated, we acylated and alkylated compound **12** with benzoyl chloride and benzyl bromide, respectively, to give **16** and **17** as crystalline solids.

## Results and Discussion

**Design.** We noticed that the three aromatic rings of **1** (Figure 1) in the CDK2-bound forms were almost exactly coplanar in practically all cases (Figure 2a).[19,20] This flat inhibitor shape is presumably dictated by the narrow cleft-like shape of the CDK2 ATP-binding site. Molecular dynamics simulations with **1** suggest that in low-energy inhibitor solution conformations such as that shown in Figure 2b the planes of the thiazole and the pyrimidine rings are not coincident because of steric repulsion between the thiazol-4-ylmethyl group and the pyrimidine C5-H. As a result, **1** must pay both an enthalpic and entropic price in order to adopt the bioactive coplanar conformation.

Furthermore, in rotamer conformations such as that shown in Figure 2a, the thiazol-4-yl methyl group is ideally positioned to interact with the aromatic ring side chain of F80 in CDK2; identical or similar aromatic side chains are found at this so-called gatekeeper position in other CDKs,[16] and this presumably constitutes a kinase selectivity determinant in the thiazolopyrimidine pharmacophore. It thus occurred to us to lock the relative orientations of the thiazole and pyrimidine rings into the bioactive one by introducing the conformational constraint shown in **2** (Figure 1), i.e., by tethering the thiazol-4-ylmethyl to the pyrimidine C5 atom through a methylene bridge (Figure 2c). This constraint was hypothesized to increase the potency of the nonconstrained analogues for CDK2 in a 3-fold manner: (1) it would serve to decrease the entropic cost of binding by restricting the freedom of the rotatable bond between the thiazole and pyrimidine rings; (2) it would remove the clash between the thiazol-4-ylmethyl group and the pyrimidine C5-H mentioned above, resulting in more favorable intramolecular energies, and (3) addition of the dimethylene bridge between the two rings would provide additional van der Waals contacts to the CDK2 binding pocket. Unlike the coplanarity of the thiazole and pyrimidine rings, coincidence of the planes of the pyrimidine and aniline rings as observed in CDK2-bound inhibitor compound conformations (Figure 2a) is expected to be more favorable. This fact lies at the heart of the success of the 2-anilinopyrimidine, as opposed, for example, to the 2-anilinopyridine template (where clashing of an aniline ortho-proton with the pyridine C3-H prevents coplanarity) in kinase inhibitor pharmacophores.[30] These facts are also supported by single-crystal structures we obtained for 2-anilino-4-(2,4-dimethylthiazol-5-yl)pyrimidine **1b**[20] and compound **11g** (Figure 2e and Figure 2f). An overlay of the single-crystal and CDK2 complex crystal structures (see below for discussion) of these unconstrained (**1b** and 4-(2,4-dimethylthiazol-5-yl)-*N*-(3-nitrophenyl)pyrimidin-2-amine **1c**)[20] and constrained (**11g**) compounds illustrates that the conformations differ considerably more in the former than the latter case (Figure 2d).

**CDK2 Binding Mode.** The X-ray crystal structure of compound **11g** (Table 1) bound to the CDK2−cyclin A complex shows that the inhibitor occupies the ATP-binding cleft between the two lobes of the kinase subunit (Figure 3a). Overall the binding mode of **11g** is very similar to those we have previously described for unconstrained thiazolopyrimidine CDK inhibitors.[19−22] The aminopyrimidine part of the inhibitor occupies the adenine subsite of the ATP-binding pocket, whereas the thiazole portion projects into the ribose subsite. The nitroaniline system binds in the cleft at the opening of the ATP-binding pocket, and the nitro group forms intimate electrostatic interactions with polar residues lining the entrance to this cleft. The usual H-bonds between the CDK2 hinge region and L83 (carbonyl and NH) backbone and the inhibitor aminopyrimidine system is observed (Figure 3b).[19] As mentioned above, the design of the constrained thiazolopyrimidine pharmacophore based on docking experiments suggested that introduction of an additional $CH_2$ unit would result in better van der Waals contacts with the F80 gatekeeper. The complex crystal structure confirms this, and the F80 side chain, especially at the $C^{\beta}$ position, packs closely against the methylene bridge (Figure 3b).

**Computational Analysis.** In order to investigate the impact of the cyclic constraint upon binding relative to the noncyclized analogues in more depth, energetic calculations were performed on **1c** and **11g**, which are identical with the exception of the constraint. In the first instance, the ligand conformations were extracted from their respective CDK2 complex crystal structures and were then energy minimized. The difference in intramolecular energy was compared between the bound and energy-minimized forms of both inhibitors. The results of these calculations demonstrate that in order for the unconstrained analogue **1c** to make effective contacts with the CDK2 binding pocket, it must adopt a nonoptimal high energy conformation (Table 2). The constrained derivative **11g**, on the other hand, undergoes a smaller energy transition, indicating that the constraint

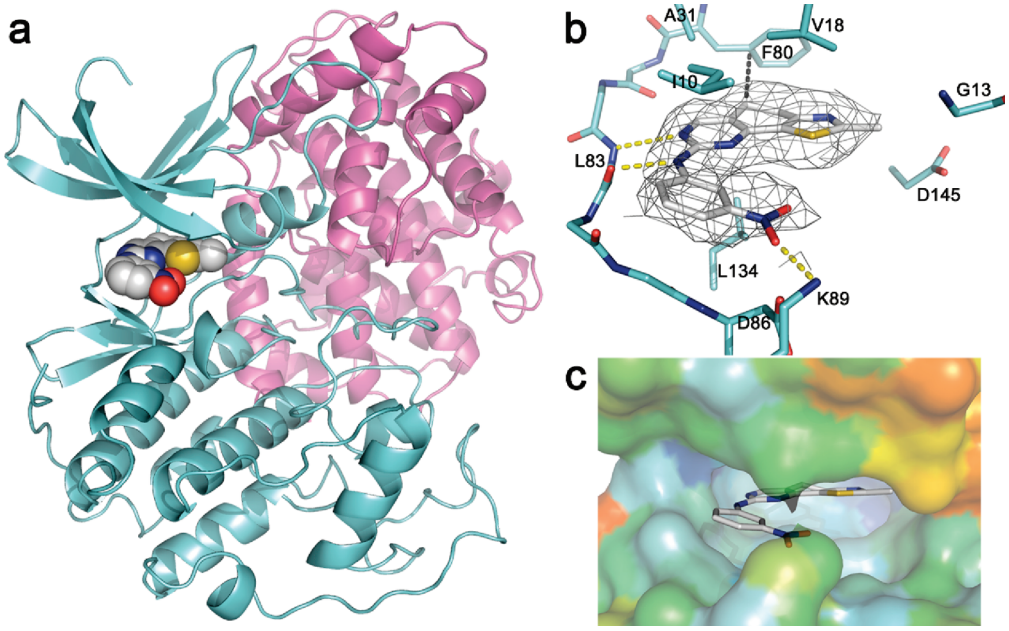


**Figure 3.** (a) Compound **11g** (space-filled CPK model) occupies the ATP-binding cleft of CDK2 (cyan ribbon) in the X-ray crystal structure complex with cyclin A (magenta ribbon). (b) Only residues within 4 Å of bound **11g** (with the mesh indicating the electron density, contoured at 0.5$\sigma$, observed in the crystal structure) are shown, including the hinge region (F80−D86). H-Bonds with L83 and hydrophobic interaction with the gatekeeper residue F80 are indicated by broken lines. (c) The binding pose of **11g** in CDK2 (surface with B-factor coloring).

**Table 2.** Energetic Comparison of Nonconstrained and Constrained Thiazolopyrimidine CDK Inhibitors[a]

| | compd | |
|---|---|---|
| | **1c** | **11g** |
| CDK2−cyclin E inhibition, $IC_{50}$ ($\mu$M) | 0.11 | 0.023 |
| CDK2-bound intramolecular energy | 194 | 189 |
| free intramolecular energy | 65 | 94 |
| difference between bound and free intramolecular difference | 129 | 95 |
| van der Waals interaction energy | −14 | −46 |
| total interaction energy | −31 | −55 |

[a] Energies in kcal/mol.

minimizes the enthalpic cost of binding. Apart from the intramolecular analysis, calculation of protein−ligand interaction energies from the CDK2 crystal structures provides additional evidence that the binding is more favorable in the context of the constrained analogue and results from greater complementarity with the hydrophobic parts of the binding pocket (Table 2). Neither of these calculations accounts for entropic factors, and therefore, the restriction of the rotatable bond between the thiazole and the pyrimidine rings is an additional component of the 4.5-fold increase in potency (affinity) observed for the constrained analogue **11g** relative to **1c**.

**SARs.** The parent analogue **11a**, which contains an unsubstituted aniline system, is a very potent CDK2 inhibitor. Furthermore, it is substantially selective for CDK2, as the other four CDK complexes assessed in this study were inhibited with at least 200-fold lower potency (Table 1). Interestingly, the introduction of aniline substituents in many cases preserved potency but resulted in different selectivity profiles. Thus, the *m*-hydroxy compound **11d**, while about 10-fold less potent than **11a** against CDK2, is comparatively more potent with respect to CDK7 and CDK9, whereas the *p*-hydroxy isomer **11e** has a similar potency and selectivity profile as **11a**. A similar picture is seen with the *m*-nitro analogues **11g** and **11h**, where selectivity with respect to CDK7, and especially CDK9, is enhanced much more than with the *p*-nitro derivative **11f**. Overall, analogue design in the present constrained thiazolopyrimidine series was guided by our earlier results with the corresponding unconstrained compounds.[20] There we observed that the presence of electron-withdrawing groups in the aniline meta or para positions, especially when combined with an $NH_2$ group at the thiazole C2 position, afforded very potent compounds. Here we observed that the thiazol-2-ylamino versus -methyl group (**11b** versus **11a**) reduced CDK2 inhibitory potency strongly but marginally enhanced potency with respect to the other CDKs. When combined with the aniline *m*-nitro substituent (**11h** versus **11g**), however, introduction of the thiazol-2-ylamino strongly enhanced activity with respect to CDK1 and CDK2. A similar enhancing effect of the thiazol-2-ylamino group on CDK1 potency was observed in connection with the *p*-dimethylaminoaniline group (**11n** versus **11i**). In general, comparatively large substituents at the aniline para position (**11j** and **11m**) were poorly tolerated in terms of activity across the board. Of the potent analogues, those in which the aniline was replaced with a 3-aminopyridine system (**11k** and **11l**) are unique insofar as they exhibited CDK1−CDK2−CDK4 versus CDK7−CDK9 selectivity. As in the corresponding unconstrained thiazolopyrimidine series, the presence of an NH-aryl substituent at the pyrimidine C2 position is crucial for CDK inhibitory activity. This can be deduced from the facts that analogue **12**, which lacks a phenyl group, and the derivatives with insertion of a carbonyl (**16**) or methylene (**17**) function between the amino and aryl groups are devoid of inhibitory activity. Furthermore, replacement of the proton in the secondary aniline function of, for example, compound **11g** with a methyl group (**14**) leads to reduction in potency by at least 100-fold with respect to all CDKs except CDK7, where the reduction is less pronounced. These findings are in line with the role of the

**Table 3.** Antiproliferative Potency of Compound **11g** against Human Tumor Cell Lines of Different Histological Origin

| tumor cell line | | |
|---|---|---|
| designation | histology | 72-h MTT $IC_{50} \pm SD$ ($\mu$M) |
| A549 | lung | $0.69 \pm 0.22$ |
| HeLa | cervix | $1.1 \pm 0.1$ |
| HT-29 | colon | $1.4 \pm 0.3$ |
| MCF-7 | breast | $1.7 \pm 0.1$ |
| Saos-2 | bone | $1.2 \pm 0.7$ |

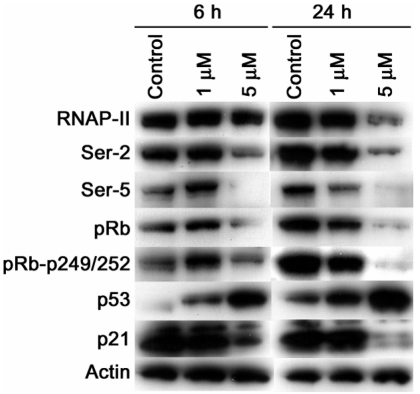


**Figure 4.** Western blot analysis of A2780 tumor cell extracts following treatment with compound **11g**.

aniline NH group as a key H-bond donor in the observed binding mode of, for example, **11g** (Figure 3c). The fully aromatic compound **15b** was observed to be substantially less potent than its counterpart with a partially saturated central six-membered ring (**11a**), but again methylation of the aniline NH (compound **15a**) practically abolished inhibitory activity.

In summary, the constrained thaizolopyrimidines in Table 1 are generally more potent than the corresponding unconstrained derivatives, but they possess subtly different selectivity profiles. For example, **11a** is substantially more potent than the corresponding unconstrained counterpart with respect to CDK2, but the differences are less pronounced as far as the other CDKs are concerned (the unconstrained analogue, compound **11**, in ref 20, has $K_i$ values of 0.51, 0.08, 2.6, 5.4, and 0.56 $\mu$M for CDK1, CDK2, CDK4, CDK7, and CDK9, respectively), whereas **11h** is marginally more potent than its unconstrained parent but possesses a similar selectivity profile (the unconstrained analogue, compound **32** in ref 20, has $K_i$ values of 0.08, 0.002, 0.053, 0.070, and 0.004 $\mu$M for CDK1, CDK2, CDK4, CDK7, and CDK9, respectively).

**Cellular Mode of Action of Prototype Compound.** We chose compound **11g** as the prototype from the constrained thiazolopyrimidine series for cell-based studies. The antiproliferative potency of this compound against a range of different human tumor cell lines of different histological origin is summarized in Table 3. Compound **11g** induced a response in cancer cells consistent with suppression of transcription through CDK inhibition (Figure 4). At the 6 h time point, 5 $\mu$M **11g** significantly reduced the phosphorylation of RNAP-II at the Ser-2 and Ser-5 residues of the CTD (CDK7 and CDK9 phosphorylation sites) without changes to the total amount of RNAP-II. Total retinoblastoma protein (pRb) was reduced at the same time point and concentration, and no conclusions can therefore be drawn regarding cellular

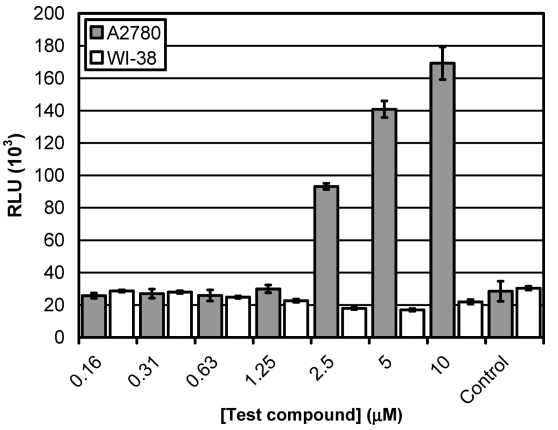


**Figure 5.** Selective induction of apoptosis, as assessed by measurement of caspase-3 and -7 activity in tumor (A2780) and untransformed (WI-38) proliferating cells following treatment for 24 h with compound **11g**.

inhibition of cell-cycle CDKs that act on pRb (mainly CDK2 and CDK4). There was a pronounced increase in p53 protein levels as a result of treatment with **11g**, which we ascribe to the transcriptional down-regulation of the short-lived negative p53 regulator Mdm2.[34] However, p53 induction did not result in a subsequent increase in the transcription of p21, which is normally regulated by p53; again, this is consistent with a reduction in transcriptional activity of the treated cells. The antiproliferative effect of **11g** appears to be a consequence of activation of the cellular apoptosis program. Furthermore, compound **11g** selectively induces apoptosis in transformed cells. Caspase-3/7 activity was measured after 24 h of treatment of nontransformed proliferating WI-38 fibroblasts or transformed ovarian A2780 tumor cells with compound **11g** (Figure 5). There was a strong induction of caspase activity in the transformed line at concentrations as low as 2.5 $\mu$M and greater, with no caspase activity detected in the nontransformed line. Flow cytometric analysis of treated transformed and nontransformed cells reinforces this picture (Figure 6) and further shows that apoptotic cells emanate from all rather than any individual cell cycle compartments. This result suggests that the antiproliferative effect of compound **11g** is due to its inhibition of CDK regulation of transcription rather than the cell cycle.

## Conclusions

Starting from our previous results with 2-anilino-4-(thiazol-5-yl)pyrimidine CDK inhibitors **1**,[20] we have designed, synthesized, and characterized ring-constrained derivatives, i.e., 2-amino-*N*-aryl-4,5-dihydrothiazolo[4,5-*h*]quinazolin-8-amines **2**. Overall, similarities were observed between the unconstrained and constrained inhibitor series in terms of SARs. Both series contain very potent CDK inhibitors, although there were subtle differences in the CDK selectivity profiles between the series.

## Experimental Methods

Chemical reagents and solvents were obtained from commercial sources. When necessary, solvents were dried and purified by standard methods. Thin-layer chromatography was performed using glass plates coated with silica gel; developed plates were air-dried and analyzed under a UV lamp (254/365 nm). Flash column chromatography[35] was performed using Fluorochem silica gel (35−70 $\mu$m). Magnesium sulfate was used as a drying agent for

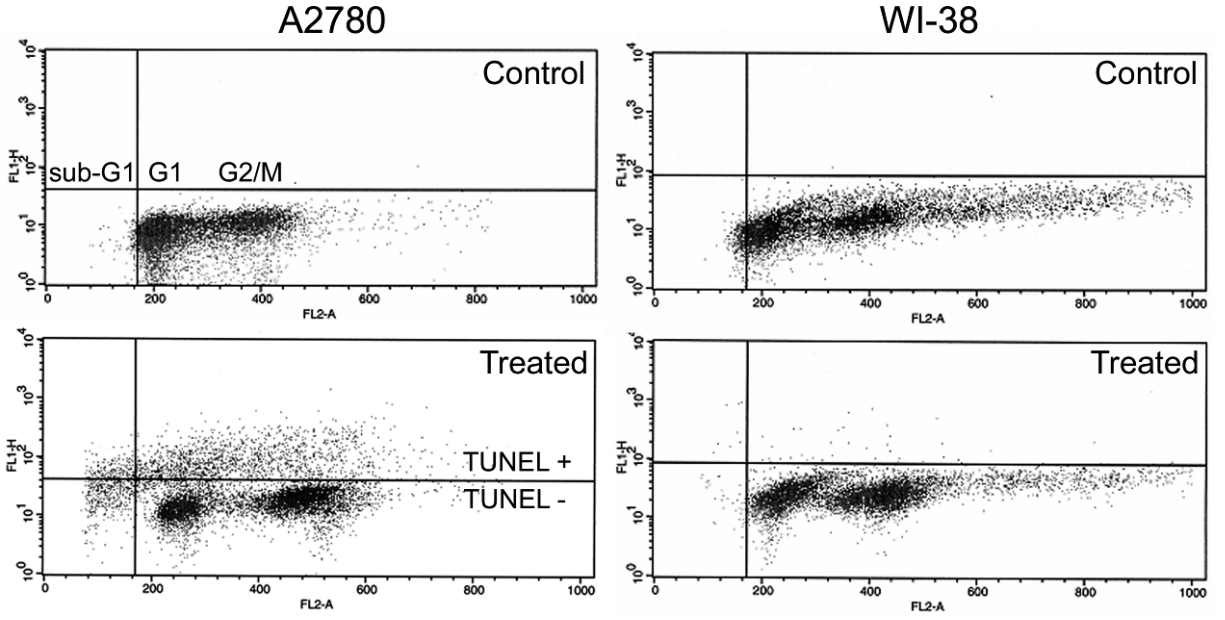


**Figure 6.** Selective induction of apoptosis in transformed cells. Flow cytometric analysis was performed, and apoptosis (by TUNEL assay gating, ordinate) was correlated with cell cycle stage (by DNA content gating; abscissa). A2780 cancer cells and WI-38 normal cells (indicated) were treated with assay diluent only (labeled, control) or with 5 $\mu$M compound **11 g** (labeled, treated) for 24 h. Treatment with compound **11g** (5 $\mu$M) resulted in 20% TUNEL-positive A2780 cells, whereas similar treatment of WI-38 cells gave rise to only 0.7% TUNEL-positive cells.

organic solutions. Melting points were determined with an Electrothermal 9100 capillary melting point apparatus and are uncorrected. NMR spectra were recorded on a Bruker Avance 300 spectrometer ($^1$H, 300 MHz; $^{13}$C, 75.5 MHz), using the residual solvent as the internal reference in all cases. Assignments of $^{13}$C resonances were made, where possible, using the PENDANT sequence. Elemental microanalyses and high resolution mass spectrometry were performed within the School of Chemistry, University of St. Andrews, U.K. Target compounds for which elemental microanalysis was not obtained or for which analytical results obtained were not within 0.4% of calculated values were further analyzed using two different RP-HPLC systems: linear gradient elution using $H_2O$/MeCN (containing 0.1% $CF_3COOH$) or $H_2O$/MeOH (containing 0.1% $CF_3CO$-OH). In both cases a flow rate of 1 mL/min and a gradient elution time of 25 min, using a Phenomenex Synergi 4u Hydro-RP 80A (150 mm × 4.6 mm) column and a diode array detector, were used. Compound purities by RP-HPLC were ≥95% throughout.

**2-Acetamido-6-(hydroxymethylene)-5,6-dihydro-4*H*-benzothiazol-7-one (8b).** A mixture of **7c** (3.0 g, 14.3 mmol) and NaOMe (15.5 g, 286 mmol) in dry THF (100 mL) was stirred at room temperature for 15 min under a $N_2$ atmosphere. The reaction mixture was cooled in an ice bath before freshly distilled ethyl formate (21.2 g, 286 mmol) was added dropwise. The mixture was brought to room temperature and stirred for 5 h. Evaporation of the solvent gave a yellow solid which was dissolved in water (100 mL). The solution was carefully acidified to pH 5 (conc HCl) and was extracted with EtOAc (3 × 100 mL). The combined organic extracts were dried and concentrated under vacuum to afford **8b** as a yellow solid (3.11 g, 91%): mp 213−215 °C. $^1$H NMR (DMSO-$d_6$): $\delta$ 12.52 (s, 1H, NH), 10.83 (d, 1H, *J* 6.4, OH), 7.57 (d, 1H, *J* 6.4, CH), 2.88−2.69 (m, 4H, $CH_2$-$CH_2$), 2.18 (s, 3H, $COCH_3$). $^{13}$C NMR (DMSO-$d_6$): $\delta$ 182.0 (C), 169.1 (C), 162.1 (C), 161.4 (C), 151.3 (CH), 124.8 (C), 110.8 (C), 25.3 ($CH_2$), 22.6 ($CH_3$), 20.5 ($CH_2$). HRMS (EI): *m*/*z* $[M]^+$ calcd for $C_{10}H_{10}N_2O_3S$ 238.0412, found 238.0407.

**2-Methyl-6-(morpholinomethylene)-5,6-dihydro-4*H*-benzothiazol-7-one (9a).** To a solution of **8a** (2.00 g, 10.2 mmol) in PhMe (30 mL), morpholine (0.97 g, 11.2 mmol) was added. The reaction mixture was heated under reflux for 2 h. Evaporation of the solvent gave a brown crude solid, which was purified by flash column chromatography (EtOAc−hexane) to afford **9a** as a yellow solid (2.35 g, 87%). Analytically pure product was obtained after crystallization from EtOH: mp 186−187 °C. Anal. RP-HPLC: $t_R$ = 12.7 min (0−60% MeCN, purity 100%). $^1$H NMR (DMSO-$d_6$): $\delta$ 7.34 (s, 1H, CH), 3.66−3.60 (m, 4H, 2 × $CH_2$), 3.52−3.46 (m, 4H, 2 × $CH_2$), 2.94−2.81 (m, 4H, $CH_2$-$CH_2$), 2.66 (s, 3H, $CH_3$). $^{13}$C NMR ($CDCl_3$): $\delta$ 182.0 (C=O), 171.6 (C), 162.3 (C), 147.9 (CH), 133.2 (C), 103.3 (C), 67.0 (2 × $CH_2$), 51.5 (2 × $CH_2$), 26.8 ($CH_2$), 25.0 ($CH_2$), 20.3 ($CH_3$). HRMS (CI): *m*/*z* $[M + H]^+$ calcd for $C_{13}H_{17}N_2O_2S$ 265.1010, found 265.1007.

**2-Acetamido-6-(morpholinomethylene)-5,6-dihydro-4*H*-benzothiazol-7-one (9b).** To a suspension of **8b** (2.5 g, 10.5 mmol) in PhMe (40 mL), morpholine (1.00 g, 11.5 mmol) was added. The reaction mixture was heated under reflux for 2 h. After the mixture was cooled, the dark-yellow precipitate was collected, washed with EtOH, and dried to afford **9b** as a yellow solid (2.86 g, 89%). Analytically pure product was obtained after crystallization from EtOH: mp ∼240 °C (dec). $^1$H NMR (DMSO-$d_6$): $\delta$ 12.37 (br s, 1H, NH), 7.28 (s, 1H, CH), 3.66−3.59 (m, 4H, 2 × $CH_2$), 3.49−3.42 (m, 4H, 2 × $CH_2$), 2.93−2.75 (m, 4H, $CH_2$-$CH_2$), 2.16 (s, 3H, $COCH_3$). $^{13}$C NMR (DMSO-$d_6$): $\delta$ 181.0 (C=O) 169.3 (C), 161.5 (C), 158.8 (C), 146.9 (CH), 125.6 (C), 102.1 (C), 66.5 (2 × $CH_2$), 50.9 (2 × $CH_2$), 26.0 ($CH_2$), 24.0 ($CH_2$), 23.0 ($CH_3$). HRMS (EI): *m*/*z* $[M]^+$ calcd for $C_{14}H_{17}N_3O_3S$ 307.0991, found 307.0999.

**General Procedure for the Preparation of *N*-Arylguanidine Salts (10).** The preparation of *N*-arylguanidine nitrate and hydrochloride salts has been described previously.[20,30,31]

**General Procedure for the Preparation of 2-Methyl- and 2-Amino-*N*-aryl-4,5-dihydrothiazolo[4,5-*h*]quinazolin-8-amine (11, $R^1$ = Me and $NH_2$). Method A.** A mixture of **9a** or **9b** (1 equiv), the appropriate *N*-arylguanidine salt (**10**, 2 equiv) and NaOH (2 equiv) in 2-methoxyethanol was heated at 125 °C for 22 h. After the mixture was cooled, the solvent was evaporated and the residue was purified by flash column chromatography using appropriate mixtures of EtOAc and hexane as the eluant. The products were further purified by crystallization from appropriate solvents.

**2-Methyl-4,5-dihydrothiazolo[4,5-*h*]quinazolin-8-amine (12).** A mixture of **9a** (2.24 g, 8.47 mmol), guanidine hydrochloride (0.89 g, 9.32 mmol), and NaOH (0.37 g, 9.32 mmol) in EtOH (100 mL) was heated under reflux for 4 h. Evaporation of the solvent gave a brown solid which was purified by flash column chromatography through a bed of silica using 10% MeOH−EtOAc as the eluant. The product **12** was obtained as a yellow solid (1.66 g, 90%): mp 241−243 °C. Anal. RP-HPLC: $t_R$ = 8.7 min (0−60% MeCN, purity 100%). $^1$H NMR (DMSO-$d_6$): $\delta$ 8.08 (s, 1H, pyrimidine-H), 6.51 (br s, 2H, $NH_2$), 2.98−2.80 (m, 4H, $CH_2$-$CH_2$), 2.69 (s, 3H, $CH_3$). $^{13}$C NMR (DMSO-$d_6$): $\delta$ 168.0 (C), 162.7 (C), 158.4 (C), 155.9 (C), 155.7 (CH), 128.1 (C), 113.6 (C), 24.9 ($CH_2$), 23.0 ($CH_2$), 19.4 ($CH_3$). HRMS (EI): $m/z$ $[M]^+$ calcd for $C_{10}H_{10}N_4S$ 218.0626, found 218.0618.

**General Procedure for the Preparation of 2-Methyl-*N*-aryl-4,5-dihydrothiazolo[4,5-*h*]quinazolin-8-amine (11, R$^1$ = Me). Method B.** To a dry resealable Schlenk tube purged with $N_2$ was added **12** (218 mg, 1.0 mmol), $Cs_2CO_3$ (456 mg, 1.4 mmol), xantphos ligand (3.2 mg, L/Pd = 1.1), and the appropriate aryl bromide **13** (1.0 mmol) under a stream of $N_2$. $Pd_2(dba)_3$ (4.6 mg, 1 mol %) in dry 1,4-dioxane (3 mL) was added via cannulation. The Schlenk tube was capped and carefully subjected to three cycles of evacuation−backfilling with $N_2$. The tube was sealed and immersed in a 115 °C oil bath for 16 h. After the mixture was cooled, the solvent was evaporated and the residue was purified by flash column chromatography using appropriate mixtures of EtOAc and hexane as the eluant. The products were further purified by crystallization from appropriate solvents.

**2-Methyl-*N*-phenyl-4,5-dihydrothiazolo[4,5-*h*]quinazolin-8-amine (11a). 11a** was obtained from **9a** and **10** ($R^2$ = $R^3$ = H, X = CH) by method A. Cream solid (46%). **11a** was obtained from **12** and **13** ($R^2$ = $R^3$ = H) by method B (71%): mp 223−224 °C. Anal. RP-HPLC: $t_R$ = 16.0 min (0−60% MeCN, purity 100%), $t_R$ = 17.3 min (0−60% MeOH, purity 100%). $^1$H NMR ($CDCl_3$): $\delta$ 8.19 (s, 1H, pyrimidine-H), 7.67−7.61 (m, 2H, *o*-Ph-H), 7.37−7.29 (m, 2H, *m*-Ph-H), 7.27 (br s, 1H, NH), 7.05−6.98 (m, 1H, *p*-Ph-H), 3.12−2.92 (m, 4H, $CH_2$-$CH_2$), 2.76 (s, 3H, $CH_3$). $^{13}$C NMR ($CDCl_3$): $\delta$ 169.5 (C), 159.2 (C), 159.1 (C), 157.0 (C), 155.2 (CH), 139.8 (C), 129.0 (CH), 128.8 (C), 122.2 (CH), 118.9 (CH), 116.6 (C), 25.4 ($CH_2$), 24.0 ($CH_2$), 19.9 ($CH_3$). HRMS (EI): $m/z$ $[M]^+$ calcd for $C_{16}H_{14}N_4S$ 294.0939, found 294.0947.

**2-Methyl-*N*-(3-(nitro)phenyl)-4,5-dihydrothiazolo[4,5-*h*]quinazolin-8-amine (11g). 11g** was obtained from **9a** and **10** ($R^2$ = $NO_2$, $R^3$ = H, X = CH) by method A. Yellow solid (5%). **11g** was obtained from **12** and **13** ($R^2$ = $NO_2$, $R^3$ = H) by method B (83%). Crystals suitable for X-ray analysis were obtained from AcOH (see Supporting Information): mp 227−228 °C. Anal. RP-HPLC: $t_R$ = 21.9 min (0−60% MeCN, purity 100%). $^1$H NMR (DMSO-$d_6$): $\delta$ 10.08 (s, 1H, NH), 8.95 (dd, 1H, *J* 2.3, 2.3, Ar-H), 8.35 (s, 1H, pyrimidine-H), 8.00 (ddd, 1H, *J* 8.2, 2.3, 0.8, Ar-H), 7.74 (ddd, 1H, *J* 8.2, 2.3, 0.8, Ar-H), 7.52 (dd, 1H, *J* 8.2, 8.2, Ar-H), 3.04−2.90 (m, 4H, $CH_2$-$CH_2$), 2.71 (s, 3H, $CH_3$). $^{13}$C NMR (DMSO-$d_6$): $\delta$ 169.2 (C), 159.3 (C), 158.4 (C), 156.0 (C), 155.4 (CH), 148.0 (C), 142.0 (C), 129.6 (CH), 127.6 (C), 124.2 (CH), 117.1 (C), 115.2 (CH), 111.9 (CH), 24.6 ($CH_2$), 23.1 ($CH_2$), 19.5 ($CH_3$). HRMS (EI): $m/z$ $[M]^+$ calcd for $C_{16}H_{13}N_5O_2S$ 339.0789, found 339.0797.

***N*,2-Dimethyl-*N*-(3-nitrophenyl)-4,5-dihydrothiazolo[4,5-*h*]quinazolin-8-amine (14).** Under dry conditions NaH (7.9 mg, 0.33 mmol) was added to a solution of **11g** (102 mg, 0.3 mmol) in dry DMF (2 mL). After effervescence had subsided, iodomethane (51 mg, 0.36 mmol) was added dropwise and the reaction mixture was stirred at room temperature for 16 h. The solvent was removed, water was added (20 mL), and the product was extracted with $CH_2Cl_2$ (3 × 30 mL). The combined extracts were dried, filtered, and concentrated under vacuum. Flash column chromatography (EtOAc−hexane) afforded **14** as a yellow solid (40 mg, 38%): mp 203−204 °C. Anal. RP-HPLC: $t_R$ = 17.1 min (10−70% MeCN, purity 100%). $^1$H NMR ($CDCl_3$): $\delta$ 8.36 (dd, 1H, *J* 2.3, 2.3, Ar-C2H), 8.17 (s, 1H, pyrimidine-H), 8.01 (ddd, 1H, *J* 8.2, 2.3, 1.0, Ar-H), 7.72 (ddd, 1H, *J* 7.9, 2.3, 0.8, Ar-H), 7.52 (dd, 1H, *J* 8.2, 8.2, Ar-C5H), 3.64 (s, 3H, N-$CH_3$), 3.12−2.93 (m, 4H, $CH_2$-$CH_2$), 2.75 (s, 3H, $CH_3$). $^{13}$C NMR ($CDCl_3$): $\delta$ 169.6 (C), 160.4 (C), 159.0 (C), 156.8 (C), 155.0 (CH), 148.4 (C), 146.4 (C), 131.1 (CH), 129.0 (CH) and (C) (two signals overlapping), 120.5 (CH), 119.1 (CH), 116.3 (C), 37.8 (N-$CH_3$), 25.3 ($CH_2$), 23.9 ($CH_2$), 19.8 ($CH_3$). HRMS ($ESI^+$): $m/z$ $[M + H]^+$ calcd for $C_{17}H_{16}N_5O_2S$ 354.1025, found 354.1013. An additional product in this reaction was identified as *N*,2-dimethyl-*N*-(3-nitrophenyl)thiazolo[4,5-*h*]quinazolin-8-amine (**15a**) obtained as a yellow solid (10 mg): mp 210−211 °C. Anal. RP-HPLC: $t_R$ = 23.4 min (10−70% MeCN, purity 100%). $^1$H NMR ($CDCl_3$): $\delta$ 9.09 (s, 1H, pyrimidine-H), 8.41 (dd, 1H, *J* 2.3, 2.3, Ar-C2H), 8.09 (ddd, 1H, *J* 8.2, 2.3, 1.0, Ar-H), 7.85 (part of an AB spin system, 1H, *J* 8.7, C4-H or C5-H), 7.80 (ddd, 1H, *J* 7.9, 2.0, 0.8, Ar-H), 7.72 (part of an AB spin system, 1H, *J* 8.7, C4-H or C5-H), 7.58 (dd, 1H, *J* 8.2, 8.2, Ar-C5H), 3.78 (s, 3H, N-$CH_3$), 2.93 (s, 3H, $CH_3$). HRMS ($ESI^+$): $m/z$ $[M + H]^+$ calcd for $C_{17}H_{14}N_5O_2S$ 352.0868, found 352.0865.

**2-Methyl-*N*-phenylthiazolo[4,5-*h*]quinazolin-8-amine (15b).** A mixture of **11a** (62 mg, 0.21 mmol) and DDQ (57 mg, 0.25 mmol) in dry toluene (10 mL) was heated under reflux for 4 h. After the mixture was cooled, the solvent was evaporated and the residue was purified by flash column chromatography (EtOAc−hexane). The product **15b** was obtained as a light-yellow solid (34 mg, 56%). Crystals suitable for X-ray analysis were obtained from EtOH (see Supporting Information): mp 241−243 °C. Anal. RP-HPLC: $t_R$ = 15.1 min (0−60% MeCN, purity 100%). $^1$H NMR (DMSO-$d_6$): $\delta$ 10.11 (s, 1H, NH), 9.38 (s, 1H, pyrimidine-H), 8.02−7.96 (m, 2H, *o*-Ph-H), 7.93 (part of an AB spin system, 1H, *J* 8.7, C4-H or C5-H), 7.84 (part of an AB spin system, 1H, *J* 8.7, C4-H or C5-H), 7.40−7.32 (m, 2H, *m*-Ph-H), 7.06−6.98 (m, 1H, *p*-Ph-H), 2.91 (s, 3H, $CH_3$). HRMS ($ESI^+$): $m/z$ $[M + Na]^+$ calcd for $C_{16}H_{12}N_4NaS$ 315.0680, found 315.0677.

**Kinase Assays.** CDK and other kinase assays were carried out as previously described.[20,36] $IC_{50}$ values were calculated from 10-point dose-response curves, and apparent inhibition constants ($K_i$) were calculated from the $IC_{50}$ values and appropriate $K_{m(ATP)}$ values for the kinases in question.[37]

**MTT Cytotoxicity Assays.** Standard MTT (thiazolyl blue; 3-[4,5-dimethylthiazol-2-yl]-2,5-diphenyltetrazolium bromide) assays were performed after 72 h of treatment of the cell cultures with test compounds.

**Determination of Apoptosis.** Apoptosis was determined by either a terminal deoxynucleotidyl transferase-mediated nick end labeling (TUNEL) assay (ApoDirect BD; Becton Dickinson, Franklin Lakes, NJ), collecting data from 10 000 cells and following manufacturer's instructions, or a caspase-3/7 assay (Caspase-Glo 3/7 assay; Promega, Madison, WI), following manufacturer's instructions, with cells seeded at 10 000 per well of a 96-well plate in a total volume of 100 $\mu$L of medium per well. Assays were performed 24 h after test compound addition. Detection reagent (100 $\mu$L) was added directly to each 100 $\mu$L sample, and readings were taken after a further 30 min of incubation at room temperature.

**Western Blot Analysis.** Total protein cell lysates (10 $\mu$g) were run on SDS−PAGE (4−12% gradient) gels (Invitrogen, Carlsbad, CA) under reducing conditions. The separated proteins were electroblotted to membranes, and these were probed with antibodies specific for pRb (Becton Dickinson, Franklin Lakes, NJ), 249/252 pRb (Invitrogen, Carlsbad, CA), RNAP-II, RNAP-II Ser-2, RNAP-II Ser-5 (Covance, Princeton, NJ), p53 (Oncogene ab-6; Oncogene Research Products, San Diego, CA), p21 (Santa Cruz Biotechnology, Inc., Santa Cruz, CA), and actin (Sigma, St. Louis, MO).

**Protein Crystallography.** CDK2−cyclin A protein production, purification, crystallization, and ligand introduction were performed as previously described.[19,21,38] Data were collected at

the Grenoble (France) synchrotron facility using an ADSC Quantum4. Data processing was carried out using the programs MOSFLM[39] and SCALA[40] from the CCP4 program suite. Data showed signs of crystal radiation damage. The structures were solved by molecular replacement using MOLREP[41] and PDB entry 1OKV as the search model. ARP/wARP[42] was used for initial density interpretation and the addition of water molecules. REFMAC[43] was used for structural refinement. A number of rounds of refinement and model building with the program Quanta (Accelrys, San Diego, CA) were carried out.

**Computational Chemistry.** Calculation of protein−ligand interaction energies for inhibitors in their CDK2−cyclin A complex was performed using the AFFINITY module after addition of hydrogens and 200 steps of steepest-descent minimization with the program DISCOVER of the modeling package InsightII (Accelrys, San Diego, CA). Affinity measures the van der Waals and electrostatic intermolecular energies.

**Acknowledgment.** We thank the Royal Society for a University Research Fellowship to N.J.W., the EPSRC for funding in the CASE for New Academics Scheme (N.A.M., N.J.W.), colleagues at Cyclacel, and the staff of beamline ID 14.2 at ESRF Grenoble, France, for their assistance. We thank Dr. David Smith for his support.

**Supporting Information Available:** Synthesis and analytical details for compounds **5**, **7a**−**c**, **8a**, **11b**−**f**, **11h**−**n**, **17**, and **18**; cloning and expression of His-tagged CDK9−cyclin T1; crystallographic data for the complex between CDK2−cyclin A and compound **11g**; elemental analysis results for compounds **9a**, **11c**, **11f**, **11g**, **12**, **15b**, **16**, and **17**; X-ray crystallographic data for **1b**, **11g**, and **15b**. This material is available free of charge via the Internet at http://pubs.acs.org.

## References

(1) Oelgeschlager, T. Regulation of RNA polymerase II activity by CTD phosphorylation and cell cycle control. *J. Cell. Physiol.* **2002**, *190*, 160–169.
(2) Sherr, C. J. Cancer cell cycles. *Science* **1996**, *274*, 1672–1677.
(3) Hall, M.; Peters, G. Genetic alterations of cyclins, cyclin-dependent kinases, and Cdk inhibitors in human cancer. *Adv. Cancer Res.* **1996**, *68*, 67–108.
(4) Shapiro, G. I.; Harper, J. W. Anticancer drug targets: cell cycle and checkpoint control. *J. Clin. Invest.* **1999**, *104*, 1645–1653.
(5) Geng, Y.; Yu, Q.; Sicinska, E.; Das, M.; Schneider, J. E.; Bhattacharya, S.; Rideout, W. M.; Bronson, R. T.; Gardner, H.; Sicinski, P. Cyclin E ablation in the mouse. *Cell* **2003**, *114*, 431–443.
(6) Tetsu, O.; McCormick, F. Proliferation of cancer cells despite CDK2 inhibition. *Cancer Cell* **2003**, *3*, 233–245.
(7) Ortega, S.; Prieto, I.; Odajima, J.; Martin, A.; Dubus, P.; Sotillo, R.; Barbero, J. L.; Malumbres, M.; Barbacid, M. Cyclin-dependent kinase 2 is essential for meiosis but not for mitotic cell division in mice. *Nat. Genet.* **2003**, *35*, 25–31.
(8) Murray, A. W. Recycling the cell cycle. Cyclins revisited. *Cell* **2004**, *116*, 221–234.
(9) Price, D. H. P-TEFb, a cyclin-dependent kinase controlling elongation by RNA polymerase II. *Mol. Cell. Biol.* **2000**, *20*, 2629–2634.
(10) Ramanathan, Y.; Rajpara, S. M.; Reza, S. M.; Lees, E.; Shuman, S.; Mathews, M. B.; Pe'ery, T. Three RNA polymerase II carboxyl-terminal domain kinases display distinct substrate preferences. *J. Biol. Chem.* **2001**, *276*, 10913–10920.
(11) Watanabe, Y.; Fujimoto, H.; Watanabe, T.; Maekawa, T.; Masutani, C.; Hanaoka, F.; Ohkuma, Y. Modulation of TFIIH-associated kinase activity by complex formation and its relationship with CTD phosphorylation of RNA polymerase II. *Genes Cells* **2000**, *5*, 407–423.
(12) Michels, A. A.; Nguyen, V. T.; Fraldi, A.; Labas, V.; Edwards, M.; Bonnet, F.; Lania, L.; Bensaude, O. MAQ1 and 7SK RNA interact with CDK9/cyclin T complexes in a transcription-dependent manner. *Mol. Cell. Biol.* **2003**, *23*, 4859–4869.
(13) Pinhero, R.; Liaw, P.; Bertens, K.; Yankulov, K. Three cyclin-dependent kinases preferentially phosphorylate different parts of the C-terminal domain of the large subunit of RNA polymerase II. *Eur. J. Biochem.* **2004**, *271*, 1004–1014.
(14) Kobor, M. S.; Greenblatt, J. Regulation of transcription elongation by phosphorylation. *Biochim. Biophys. Acta* **2002**, *13*, 261–275.
(15) Majello, B.; Napolitano, G. Control of RNA polymerase II activity by dedicated CTD kinases and phosphatases. *Front. Biosci.* **2001**, *6*, D1358–D1368.
(16) Fischer, P. M.; Gianella-Borradori, A. Recent progress in the discovery and development of CDK inhibitors. *Expert Opin. Invest. Drugs* **2005**, *14*, 457–477.
(17) Koumenis, C.; Giaccia, A. Transformed cells require continuous activity of RNA polymerase II to resist oncogene-induced apoptosis. *Mol. Cell. Biol.* **1997**, *17*, 7306–7316.
(18) Fischer, P. M. The use of CDK inhibitors in oncology: a pharmaceutical perspective. *Cell Cycle* **2004**, *3*, 742–746.
(19) Wu, S. Y.; McNae, I.; Kontopidis, G.; McClue, S. J.; McInnes, C.; Stewart, K. J.; Wang, S.; Zheleva, D. I.; Marriage, H.; Lane, D. P.; Taylor, P.; Fischer, P. M.; Walkinshaw, M. D. Discovery of a novel family of CDK inhibitors with the program LIDAEUS: structural basis for ligand-induced disordering of the activation loop. *Structure* **2003**, *11*, 399–410.
(20) Wang, S.; Meades, C.; Wood, G.; Osnowski, A.; Anderson, S.; Yuill, R.; Thomas, M.; Mezna, M.; Jackson, W.; Midgley, C.; Griffiths, G.; Fleming, I.; Green, S.; McNae, I.; Wu, S.-Y.; McInnes, C.; Zheleva, D.; Walkinshaw, M. D.; Fischer, P. M. 2-Anilino-4-(thiazol-5-yl)pyrimidine CDK inhibitors: synthesis, SAR analysis, X-ray crystallography, and biological activity. *J. Med. Chem.* **2004**, *47*, 1662–1675.
(21) McInnes, C.; Wang, S.; Anderson, S.; O'Boyle, J.; Jackson, W.; Kontopidis, G.; Meades, C.; Mezna, M.; Thomas, M.; Wood, G.; Lane, D. P.; Fischer, P. M. Structural determinants of CDK4 inhibition and design of selective ATP competitive inhibitors. *Chem. Biol.* **2004**, *11*, 525–534.
(22) Wang, S.; Wood, G.; Meades, C.; Griffiths, G.; Midgley, C.; McNae, I.; McInnes, C.; Anderson, S.; Jackson, W.; Mezna, M.; Yuill, R.; Walkinshaw, M.; Fischer, P. M. Synthesis and biological activity of 2-anilino-4-(1*H*-pyrrol-3-yl)pyrimidine CDK inhibitors. *Bioorg. Med. Chem. Lett.* **2004**, *14*, 4237–4240.
(23) Lehmann, G.; Luecke, B.; Schick, H.; Hilgetag, G. 2-Substituted 7-oxo-4,5,6,7-tetrahydrobenzothiazoles. *Z. Chem.* **1967**, *7*, 422.
(24) Bell, R. P.; Davis, G. G. Kinetics of the bromination of some enols and their anions. *J. Chem. Soc.* **1965**, 353–361.
(25) Fravolini, A.; Grandolini, G.; Martani, A. New heterocyclic ring systems from α-hydroxymethylene ketones. V. Reaction of 2-methyl-6-hydroxymethylene-4,5,6,7-tetrahydrobenzothiazol-7-one with amines and amidines. *Gazz. Chim. Ital.* **1973**, *103*, 1063–1071.
(26) Fravolini, A.; Grandolini, G.; Martani, A. New heterocyclic ring systems from α-hydroxymethylene ketones. IV. Reactions of 2-methyl-6-hydroxymethylene-4,5,6,7-tetrahydrobenzothiazol-7-one with semicarbazide and thiosemicarbazide leading to pyrazoline derivatives. *Gazz. Chim. Ital.* **1973**, *103*, 1057–1062.
(27) Fravolini, A.; Grandolini, G.; Martani, A. New heterocyclic ring systems from α-hydroxymethylene ketones. III. Pyrazolobenzothiazoles and thiazolobenzoisoxazoles. *Gazz. Chim. Ital.* **1973**, *103*, 755–769.
(28) Bredereck, H.; Effenberger, F.; Botsch, H. Acid amide reactions. XLV. Reactivity of formamidines, dimethylformamide diethyl acetal (amide acetal), and bis(dimethylamino)methoxymethane (aminal ester). *Chem. Ber.* **1964**, *97*, 3397–3406.
(29) Hughes, J. L.; Liu, R. C.; Enkoji, T.; Smith, C. M.; Bastian, J. W.; Luna, P. D. Cardiovascular activity of aromatic guanidine compounds. *J. Med. Chem.* **1975**, *18*, 1077–1088.
(30) Zimmermann, J.; Caravatti, G.; Mett, H.; Meyer, T.; Mueller, M.; Lydon, N. B.; Fabbro, D. Phenylamino-pyrimidine (PAP) derivatives: a new class of potent and selective inhibitors of protein kinase C (PKC). *Arch. Pharm.* **1996**, *329*, 371–376.
(31) Katritzky, A. R.; Ostercamp, D. L.; Yousaf, T. I. The mechanisms of heterocyclic ring closures. *Tetrahedron* **1987**, *43*, 5171–5186.
(32) Yin, J.; Zhao, M. M.; Huffman, M. A.; McNamara, J. M. Pd-Catalyzed N-arylation of heteroarylamines. *Org. Lett.* **2002**, *4*, 3481–3484.
(33) Strekowski, L.; Harden, M. J.; Grubb, W. B., III; Patterson, S. E.; Czarny, A.; Mokrosz, M. J.; Cegla, M. T.; Wydra, R. L. Synthesis of 2-chloro-4,6-di(heteroaryl)pyrimidines. *J. Heterocycl. Chem.* **1990**, *27*, 1393–1400.
(34) Lu, W.; Chen, L.; Peng, Y.; Chen, J. Activation of p53 by roscovitine-mediated suppression of MDM2 expression. *Oncogene* **2001**, *20*, 3206–3216.
(35) Still, W. C.; Kahn, M.; Mitra, A. Rapid chromatographic technique for preparative separations with moderate resolution. *J. Org. Chem.* **1978**, *43*, 2923–2925.
(36) McClue, S. J.; Blake, D.; Clarke, R.; Cowan, A.; Cummings, L.; Fischer, P. M.; MacKenzie, M.; Melville, J.; Stewart, K.; Wang, S.;

Zhelev, N.; Zheleva, D.; Lane, D. P. In vitro and in vivo antitumor properties of the cyclin dependent kinase inhibitor CYC202 (*R*-roscovitine). *Int. J. Cancer* **2002**, *102*, 463–468.
(37) Cheng, Y.-C.; Prusoff, W. H. Relation between the inhibition constant ($K_i$) and the concentration of inhibitor which causes fifty per cent inhibition ($I_{50}$) of an enzymic reaction. *Biochem. Pharmacol*. **1973**, *22*, 3099–3108.
(38) Kontopidis, G.; Andrews, M. J. I.; McInnes, C.; Cowan, A.; Powers, H.; Innes, L.; Plater, A.; Griffiths, G.; Paterson, D.; Zheleva, D. I.; Lane, D. P.; Green, S.; Walkinshaw, M. D.; Fischer, P. M. Insights into cyclin groove recognition: complex crystal structures and inhibitor design through ligand exchange. *Structure* **2003**, *11*, 1537–1546.
(39) Leslie, A. G. W. Recent Changes to the MOSFLM Package for Processing Film and Image Plate Data. *Joint CCP4 + ESF-EAMCB Newsletter on Protein Crystallography*; CCP4 and ESF-EAMCB, 1992; No. 26.
(40) Evans, R. R. Data Reduction. In *Proceedings of CCP4 Study Weekend, 1993, on Data Collection & Processing*; Sawyer, L., Isaacs, N., Bailey, S., Eds.; Daresbury Laboratory, Science and Engineering Research Council UK: Warrington, U.K., 1993; pp 114−122.
(41) Vagin, A.; Teplyakov, A. MOLREP: an automated program for molecular replacement. *J. Appl. Crystallogr*. **1997**, *30*, 1022–1025.
(42) Lamzin, V. S.; Wilson, K. S. Automated refinement for protein crystallography. *Methods Enzymol*. **1997**, *277*, 269–305.
(43) Murshudov, G. N.; Vagin, A. A.; Dodson, E. J. Refinement of macromolecular structures by the maximum-likelihood method. *Acta Crystallogr*. **1997**, *D53*, 240–255.